# Angewandte Chemie

*Eine Zeitschrift der Gesellschaft Deutscher Chemiker*

## Supporting Information

# SrB$_5$O$_7$F$_3$ Functionalized with [B$_5$O$_9$F$_3$]$^{6-}$ Chromophores: Accelerating the Rational Design of Deep-Ultraviolet Nonlinear Optical Materials

*Miriding Mutailipu$^+$, Min Zhang$^+$, Bingbing Zhang, Liying Wang, Zhihua Yang, Xin Zhou, and Shilie Pan\**

anie_201802058_sm_miscellaneous_information.pdf

# Supporting Information

**Experimental Section**

**Synthesis of SrB$_5$O$_7$F$_3$.** Single crystals of SrB$_5$O$_7$F$_3$ were grown by high-temperature solution method using a NaBF$_4$ flux in a closed system. A mixture of Sr(BF$_4$)$_2$ (0.3135 g, 1.2 mmol), NaBF$_4$ (0.1318 g, 1.2 mmol), and B$_2$O$_3$ (0.2089 g, 3 mmol) were loaded into a tidy quartz tube ($\Phi$10 mm × 100 mm) and dried in high-temperature to remove the inside impurities, and the tube was flame-sealed under $10^{-3}$ Pa. The tube was heated to 600 °C in 12 h, and held at this temperature for 48 h, and then cooled to 30 °C with a rate of 1.5 °C /h. Polycrystalline samples of SrB$_5$O$_7$F$_3$ can also be obtained by the low temperature molten salt reaction based on the following reaction: 3Sr(BF$_4$)$_2$ + 14H$_3$BO$_3$ → 3SrB$_5$O$_7$F$_3$ + 5BF$_3$↑+21H$_2$O↑. A mixture of Sr(BF$_4$)$_2$ (0.3135 g, 1.2 mmol), H$_3$BO$_3$ (0.3710 g, 6 mmol) was sealed in an autoclave equipped with a teflon liner (23 mL). The autoclave was heated at 220 °C for four days and cooled to room temperature at a rate of 1.5 °C /h. Powder XRD analysis confirmed the phase purity.

**Characterization.** Powder XRD analysis was collected with a Bruker D2 PHASER diffractometer (Cu Kα radiation with $\lambda$ = 1.5418 Å, 2$\theta$ = 10 to 70°, scan step width = 0.02°, and counting time= 1 s/step). The single-crystal XRD data were collected on a Bruker SMART APEX II 4K CCD diffractometer using Mo Kα radiation ($\lambda$ = 0.71073 Å) at room temperature. Data integration, cell refinement and absorption corrections were carried out with the program SAINT.[1] The structure was solved by direct methods and refined on $F^2$ by full-matrix least-squares techniques using the program suite SHELXTL.[2] Solutions were checked for missed symmetry using PLATON.[3] Although the crystal data is good ($R_{int}$ = 0.0323) and the structure solution parameters ($R_1$ = 0.0257, $wR_2$ = 0.0562, GOF = 0.971) are reasonable, the ratio of Data / Parameter cannot be improved after several crystal data collections, which is might because of the weak collected diffraction points. Thermal gravimetric analysis (TGA) and differential scanning calorimetry (DSC) were carried out on a simultaneous NETZSCH STA 449 F3 thermal analyzer instrument in a flowing N$_2$ atmosphere, the sample was placed in Pt crucible, heated from 40 to 1000 °C at a rate of 5 °C min$^{-1}$. Infrared spectroscopy was carried out on a Shimadzu IR Affinity-1 Fourier transform infrared spectrometer in the 400-4000 cm$^{-1}$ range. Ultraviolet–visible–near infrared diffuse-reflectance

spectroscopy data in the wavelength range of 190–2600 nm were recorded at room temperature using a powder sample of $SrB_5O_7F_3$ on a Shimadzu SolidSpec-3700DUV spectrophotometer. The powder SHG tests were measured by a modified Kurtz–Perry method[4] using a Q-switched Nd: $YVO_4$ solid-state laser at 1064 and 532 nm, for visible and ultraviolet SHG, respectively. Polycrystalline samples of $SrB_5O_7F_3$ were ground and sieved into the following particle size ranges: 20−38, 38−55, 55−88, 88−105, 105−150, 150−200, and 200−250 μm. The sieved KDP and β-BBO samples were used as references. The samples were pressed between two glass slides and secured in 1 mm thick aluminum holders with an 8 mm diameter hole. Then the samples were irradiated with a pulsed laser, and the second harmonic output was separated by a narrowband pass filter and detected by a photo-multiplier tube attached to an oscilloscope. No index-matching fluid was used in any of the experiments. The $^{19}F$ and $^{11}B$ MAS NMR experiments were performed on a Bruker Avance III 500 WB (11.75 T) spectrometer operating at a frequency of 470.96 and 160.61 MHz for $^{19}F$ and $^{11}B$, respectively. A commercial DVT quadruple resonance H/F/X/Y 2.5 mm CP/MAS probe was used with a spinning frequency of 30.0 kHz. Solid-state $^{19}F$ MAS NMR spectra were recorded with a single pulse excitation using a 90 degree pulse width of 1.9 us (pi/2) and a recycle delay of 5 s to obtain quantitative results. There is no fluorine background from the H/F/X/Y probehead. $^{19}F$ chemical shifts were determined using a solid external reference, Poly(tetrafluoroethylene) (PTFE). The CF2 groups of PTFE resonate at -122 ppm relative to tetramethylsilane (TMS). $^{11}B$ MAS NMR spectra was recorded, with a single pulse excitation using a short pulse length (0.32 us) to obtain quantitative results, and a recycle delay of 10 s (the tip angle was pi/12). $^{11}B$ chemical shifts were referenced using $H_3BO_3$ 1 M in solution as an external reference (19.6 ppm). The presence of B-F bonds was checked employing $^{11}B\{^{19}F\}$-REDOR NMR spectroscopy, which enables the determination of the heteronuclear $^{11}B$-$^{19}F$ dipole coupling and hence the evaluation of internuclear distances.

**Computational methods**. The electronic structure as well as optical property calculations were performed by employing CASTEP,[5] a plane-wave pseudopotential

DFT package, with the norm-conserving pseudopotentials (NCP).[6] The Perdew-Burke-Emzerhof (PBE) functional within the generalized gradient approximation (GGA) was used.[7] The plane-wave energy cutoff was set at 850.0 eV. Self-consistent field (SCF) calculations were performed with a convergence criterion of $1\times10^{-6}$ eV/atom on the total energy. The k-point separation for each material was set as 0.04 Å$^{-1}$ in the Brillouin zone corresponding to primitive cell, resulting in Monkhorst-Pack k-point meshes of $4 \times 3 \times 4$. The empty bands were set as 3 times of valence bands in the calculation to ensure the convergence of SHG coefficients.

**Table S1.** Crystal data and structure refinements of $SrB_5O_7F_3$.

| | |
|---|---|
| Empirical formula | $SrB_5O_7F_3$ |
| Formula weight | 310.67 |
| Wavelength (Å) | 0.71073 |
| Temperature (K) | 296(2) |
| Crystal system | Orthorhombic |
| Space group | $Cmc2_1$ |
| $a$ (Å) | 10.016(6) |
| $b$ (Å) | 8.654(6) |
| $c$ (Å) | 8.103(5) |
| $Z$ | 4 |
| Volume (Å$^3$) | 702.4(8) |
| Density (calc.) (g/cm$^3$) | 2.938 |
| Absorption coefficient (mm$^{-1}$) | 7.754 |
| $F(000)$ | 584 |
| Crystal size (mm$^3$) | 0.13×0.11×0.07 |
| Theta range for data collection | 3.11 to 27.58 |
| Limiting indices | $-13 \leq h \leq 9, -11 \leq k \leq 9, -10 \leq l \leq 10$ |
| Reflections collected / unique | 2081 / 829 [R(int) = 0.0323] |
| Completeness to $\theta$=27.58 | 99.4% |
| Data / restraints / parameters | 829/1/80 |
| Goodness-of-fit on F$^2$ | 0.971 |
| Final R indices [I>2sigma(I)][a] | $R_1 = 0.0257, wR_2 = 0.0562$ |
| $R$ indices (all data)[a] | $R_1 = 0.0287, wR_2 = 0.0574$ |
| Absolute structure parameter | 0.018(14) |
| Extinction coefficient | 0.0084(8) |
| Largest diff. peak and hole (e/Å$^3$) | 0.528 and -0.568 |

[a]$R_1 = \Sigma||F_o| - |F_c||/\Sigma|F_o|$ and $wR_2 = [\Sigma w(F_o^2 - F_c^2)^2/ \Sigma wF_o^4]^{1/2}$ for $F_o^2 > 2\sigma(F_o^2)$.

**Table S2.** Atomic coordinates equivalent isotropic displacement parameters and bond valence sum (BVS) for $SrB_5O_7F_3$.

| Atoms | *Wyck.* | $x$ | $y$ | $z$ | $U_{eq}(\text{Å}^2)$ | BVS |
|---|---|---|---|---|---|---|
| Sr(1) | 4*a* | 0.5000 | 0.2577(1) | 0.7213(1) | 0.010(1) | 2.369 |
| B(1) | 8*b* | 0.3653(4) | 0.8545(5) | 0.6411(5) | 0.009(1) | 3.011 |
| B(2) | 8*b* | 0.2666(5) | 0.7337(5) | 0.8952(6) | 0.012(1) | 3.062 |
| B(3) | 4*a* | 0.5000 | 0.6734(7) | 0.8379(8) | 0.011(1) | 3.015 |
| F(1) | 8*b* | 0.3686(2) | 0.0173(3) | 0.6285(3) | 0.018(1) | 0.910 |
| F(2) | 4*a* | 0.5000 | 0.5367(3) | 0.7422(4) | 0.020(1) | 1.014 |
| O(1) | 8*b* | 0.2572(2) | 0.8122(3) | 0.7482(3) | 0.012(1) | 2.085 |
| O(2) | 4*a* | 0.5000 | 0.8067(4) | 0.7148(6) | 0.008(1) | 1.954 |
| O(3) | 8*b* | 0.3508(3) | 0.7883(4) | 0.4786(3) | 0.013(1) | 2.101 |
| O(4) | 8*b* | 0.3854(3) | 0.6776(3) | 0.9451(3) | 0.012(1) | 2.186 |

**Table S3.** Anisotropic displacement parameters ($\text{Å}^2$) for $SrB_5O_7F_3$.

| Atom | $U_{11}$ | $U_{22}$ | $U_{33}$ | $U_{23}$ | $U_{13}$ | $U_{12}$ |
|------|----------|----------|----------|----------|----------|----------|
| Sr(1) | 0.008(1) | 0.011(1) | 0.010(1) | 0.000(1) | 0.000 | 0.000 |
| B(1) | 0.006(2) | 0.008(2) | 0.012(2) | 0.002(2) | -0.004(2) | -0.001(2) |
| B(2) | 0.012(2) | 0.013(2) | 0.011(2) | -0.001(2) | 0.001(2) | -0.002(2) |
| B(3) | 0.010(3) | 0.009(3) | 0.014(3) | 0.000(2) | 0.000 | 0.000 |
| F(1) | 0.013(1) | 0.009(1) | 0.030(1) | 0.005(1) | -0.004(1) | 0.000(1) |
| F(2) | 0.029(2) | 0.010(2) | 0.020(2) | -0.006(2) | 0.000 | 0.000 |
| O(1) | 0.008(1) | 0.019(1) | 0.009(2) | 0.003(1) | 0.002(1) | 0.002(1) |
| O(2) | 0.008(2) | 0.009(2) | 0.007(2) | 0.003(2) | 0.000 | 0.000 |
| O(3) | 0.009(1) | 0.021(2) | 0.009(1) | -0.003(1) | -0.001(1) | 0.000(1) |
| O(4) | 0.008(1) | 0.015(2) | 0.012(1) | 0.004(1) | 0.001(1) | -0.001(1) |

**Table S4.** Selected bond lengths (Å) and angles (º) for $SrB_5O_7F_3$.

| Bond lengths | | Bond angles | |
|---|---|---|---|
| Sr(1)-F(2) | 2.420(3) | F(1)-B(1)-O(1) | 108.4(3) |
| Sr(1)-F(1)[#1] | 2.574(3) | F(1)-B(1)-O(3) | 109.4(3) |
| Sr(1)-F(1)[#2] | 2.574(3) | O(1)-B(1)-O(3) | 112.0(3) |
| Sr(1)-O(4)[#3] | 2.576(3) | F(1)-B(1)-O(2) | 106.1(3) |
| Sr(1)-O(4)[#4] | 2.576(3) | O(1)-B(1)-O(2) | 111.1(3) |
| Sr(1)-O(3)[#5] | 2.596(3) | O(3)-B(1)-O(2) | 109.7(4) |
| Sr(1)-O(3)[#6] | 2.596(3) | O(4)-B(2)-O(3)[#9] | 124.0(4) |
| Sr(1)-O(1)[#7] | 2.628(3) | O(4)-B(2)-O(1) | 119.9(4) |
| Sr(1)-O(1)[#8] | 2.628(3) | O(3)[#9]-B(2)-O(1) | 116.0(4) |
| B(1)-F(1) | 1.413(5) | F(2)-B(3)-O(4) | 110.6(3) |
| B(1)-O(1) | 1.435(5) | F(2)-B(3)-O(4)[#10] | 110.6(3) |
| B(1)-O(3) | 1.443(5) | O(4)-B(3)-O(4)[#10] | 105.7(4) |
| B(1)-O(2) | 1.533(5) | F(2)-B(3)-O(2) | 105.9(5) |
| B(2)-O(4) | 1.348(5) | O(4)-B(3)-O(2) | 112.1(3) |
| B(2)-O(3)[#9] | 1.370(6) | O(4)[#10]-B(3)-O(2) | 112.1(3) |
| B(2)-O(1) | 1.374(5) | F(1)-B(1)-O(1) | 108.4(3) |
| B(3)-F(2) | 1.414(7) | | |
| B(3)-O(4) | 1.440(4) | | |
| B(3)-O(4)[#10] | 1.440(4) | | |
| B(3)-O(2) | 1.525(8) | | |

Symmetry transformations used to generate equivalent atom:

**#1** -x+1,y-1,z;  **#2** x,y-1,z;

**# 3** x,-y+1,z-1/2;  **# 4** -x+1,-y+1,z-1/2;

**#5** x,-y+1,z+1/2;  **# 6** -x+1,-y+1,z+1/2;

**#7** x+1/2,y-1/2,z;  **#8** -x+1/2,y-1/2,z;

**#9** -x+1/2,-y+3/2,z+1/2;  **#10** -x+1,y,z;

**Table S5.** Properties for $SrB_5O_7F_3$ and other classic nonlinear optical materials

| | $SrB_5O_7F_3$ | $Sr_2Be_2B_2O_7$ | $KBe_2BO_3F_2$ | $\beta$-$BaB_2O_4$ | $CsLiB_6O_{10}$ |
|---|---|---|---|---|---|
| **Space group** | $Cmc2_1$ | $P\bar{6}c2$ | $R32$ | $R3C$ | $I\bar{4}2d$ |
| **$\lambda_{cutoff}$ (nm)** | < 180 (144[a]) | 155 | 147 | 185 | 180 |
| **$\lambda_{SH}$ (nm)** | 180[a] | 200[a] | 162 | 205 | 237 |
| **$d_{ij}$ (pm/V)** | $d_{31} = d_{15} = 0.91$[a]<br>$d_{32} = d_{24} = -0.37$[a]<br>$d_{33} = -0.71$[a] | $d_{22} = 1.41$[a] | $d_{11} = 0.47$ | $d_{22} = 1.60$ | $d_{36} = 0.95$ |
| **Birefringence** | 0.072@589nm[a] | 0.062@589nm[a] | 0.077@1064nm | 0.1127@1064nm | 0.049@1064nm |

[a]Calculated data by using the first principles calculation method.

**Figure S1.** The experimental and calculated XRD patterns of $SrB_5O_7F_3$.
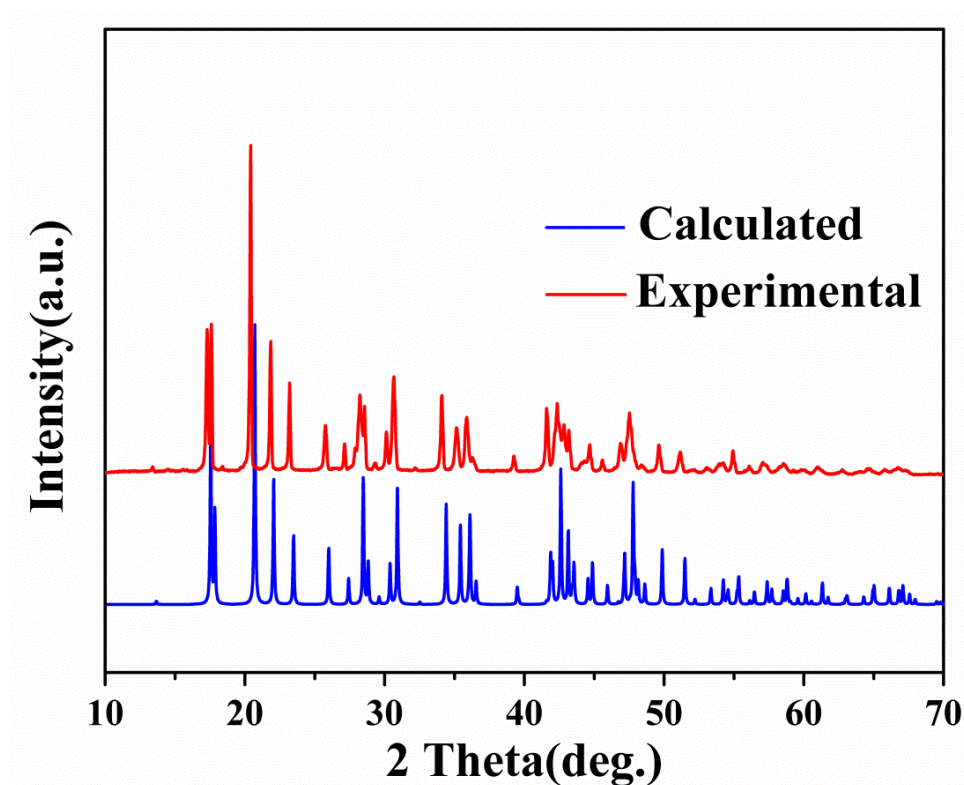


Colorless block single crystals of SBF were grown by the high-temperature solution method in a closed system. The pure polycrystalline samples of SBF can also be obtained by the low temperature molten salt reaction (Experimental procedures). The purity of the as-prepared polycrystalline samples is confirmed by the powder X-ray diffraction patterns (Figure S1)

**Figure S2.** The 18-MRs in the structure of $SrB_5O_7F_3$.
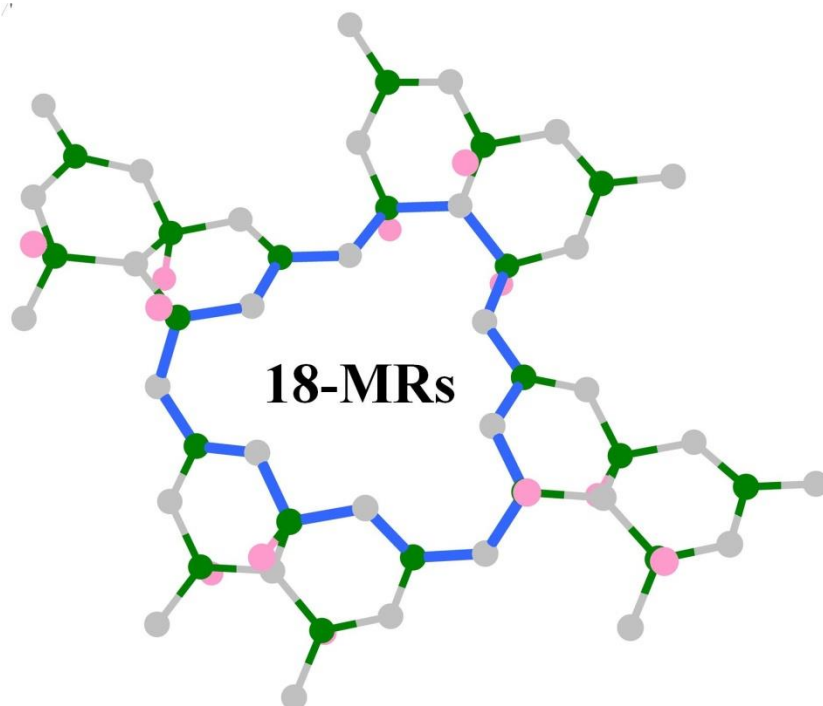


The widest and narrowest cross sections of the channels are about 6.74 and 5.16 Å, and the $Sr^{2+}$ atoms locate in the center of the 18-MR. The structural space is large enough to realize the substitutional possibility of the central $Sr^{2+}$ atoms by other alkaline-earth metal cations and the related attempts are still in progress.

**Figure S3.** The toplogical layered structures of $SrB_5O_7F_3$ in which the $[B_5O_9F_3]^{6-}$ FBBs are considered as four-connected nodes.
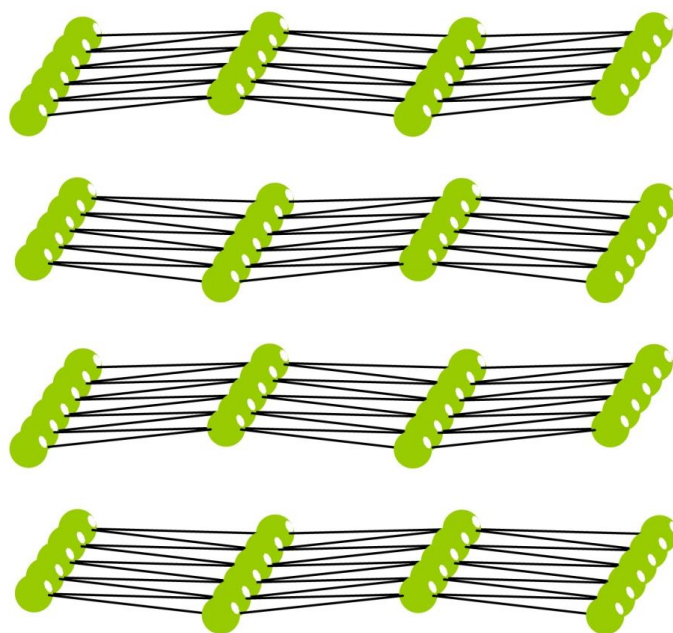


From the viewpoint of topology, the structural framework of SBF can be simplified to a four-connected (4-c) uninodal non-interpenetrated sql/Shubnikov tetragonal plane net with the Schläfli symbol of $\{4^4.6^2\}$, in which the $[B_5O_9F_3]^{6-}$ fundamental building block is considered as 4-c nodes.

**Figure S4.** The toplogical layered structures of $SrB_5O_7F_3$ viewd down in the direction of [010], the $[B_5O_9F_3]^{6-}$ FBBs are considered as four-connected nodes.
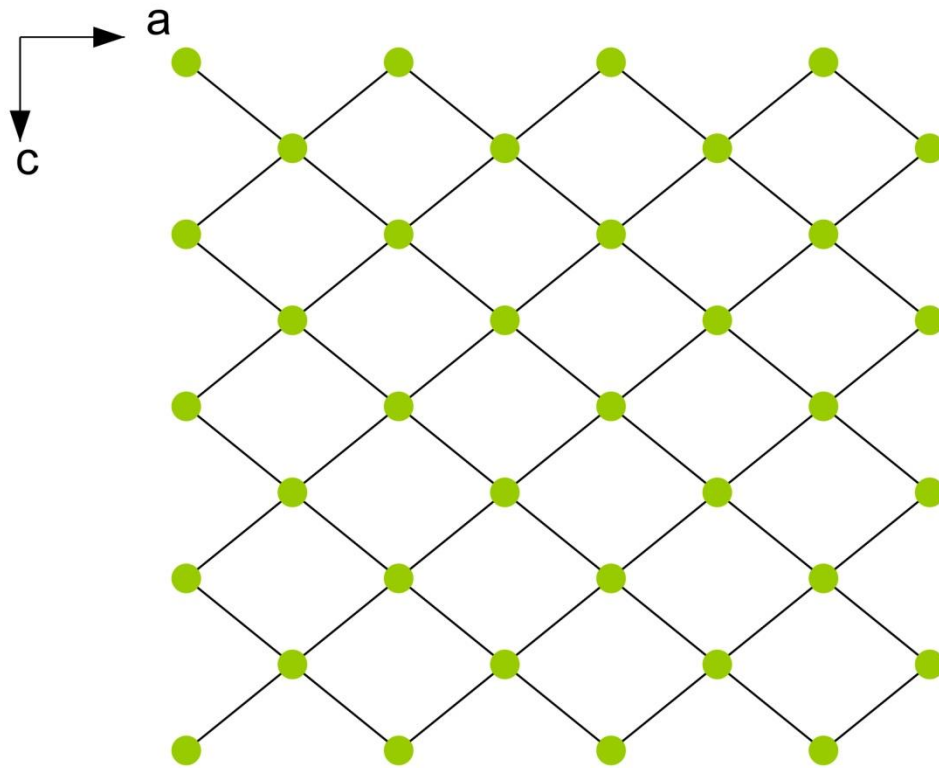
**Figure S5.** Three stereoscopic pentaborate fundamental building blocks, including $[B_5O_{10}]^{5-}$ (a), $[B_5O_{11}]^{7-}$ (b), and $[B_5O_{12}]^{9-}$ (c).
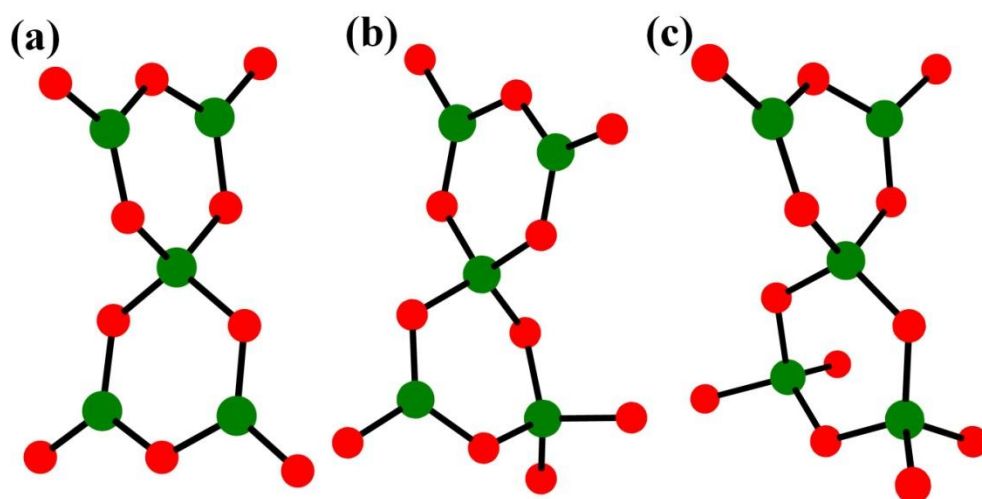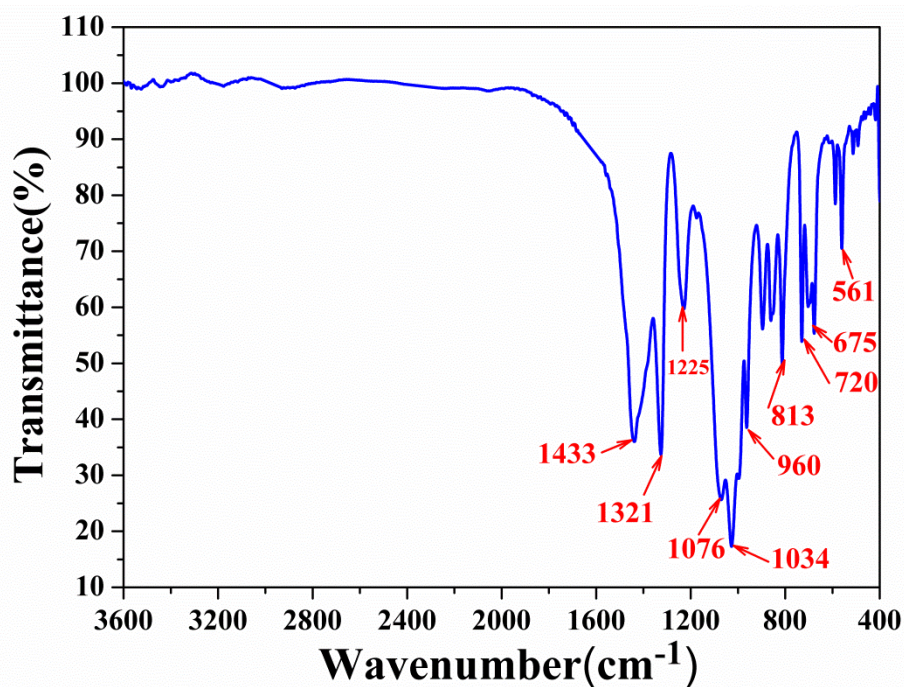
**Figure S6.** The unique $O(BO_3F)_3$ unit in the structure of $SrB_5O_7F_3$.
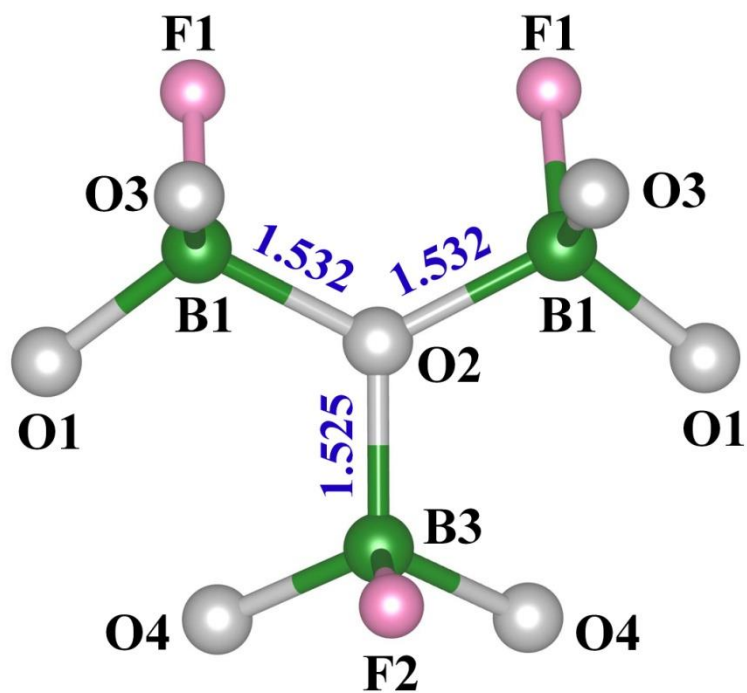


Besides, the bond valence sum calculations of central $O(2)$ atom in $O(BO_3F)_3$ results in the reasonable value of 1.954, which indicates that the unique three coordinated oxygen model is correct and feasible.

**Figure S7.** The infrared spectrum of $SrB_5O_7F_3$.



The infrared spectrum of SBF was also examined to specify the coordination model of the B atoms. The asymmetric and symmetric stretching of the $[BO_3]^{3-}$ groups are observed in 1433 and 960 $cm^{-1}$, respectively. The out-of-plane bending of the $[BO_3]^{3-}$ groups are appeared in 720 and 675 $cm^{-1}$. The peak in 561 $cm^{-1}$ corresponds to the bending of the $[BO_3]^{3-}$ group. Specially, the asymmetric stretching of the B–F bond is found in 1321 $cm^{-1}$, and the symmetric out of phase stretching of the B–F bond is also found in 813 $cm^{-1}$, this further confirms the existence of the B-F bonds in the structure of $SrB_5O_7F_3$.

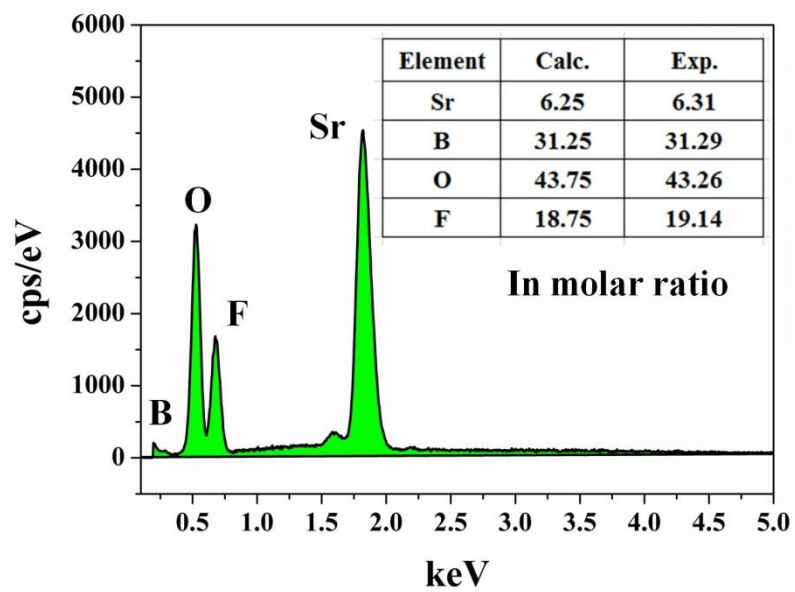**Figure S8.** Energy-dispersive X-ray spectroscopy of $SrB_5O_7F_3$.



| Element | Calc. | Exp. |
|---------|-------|-------|
| Sr | 6.25 | 6.31 |
| B | 31.25 | 31.29 |
| O | 43.75 | 43.26 |
| F | 18.75 | 19.14 |

In molar ratio

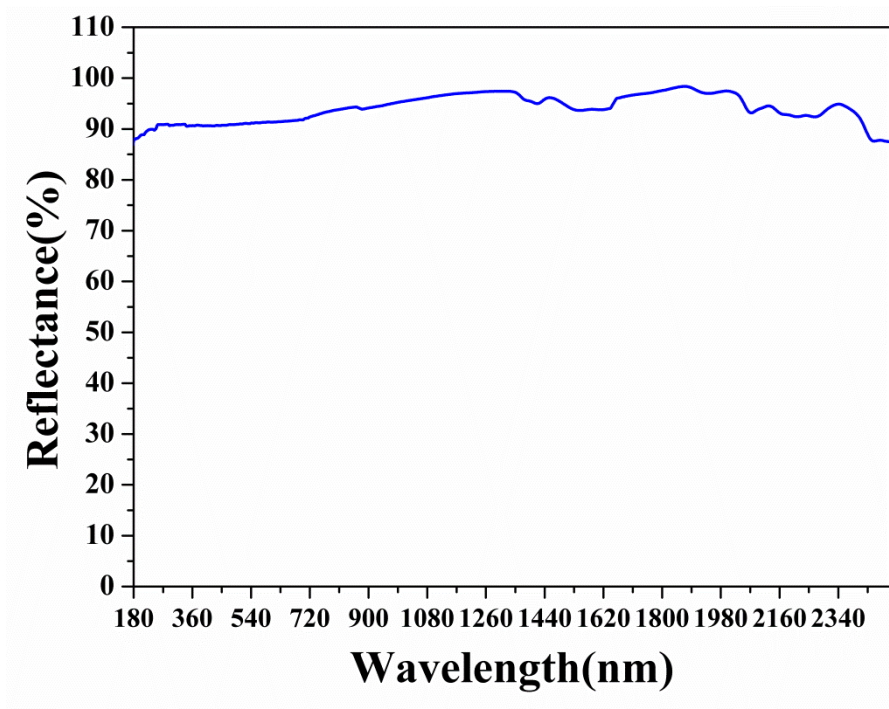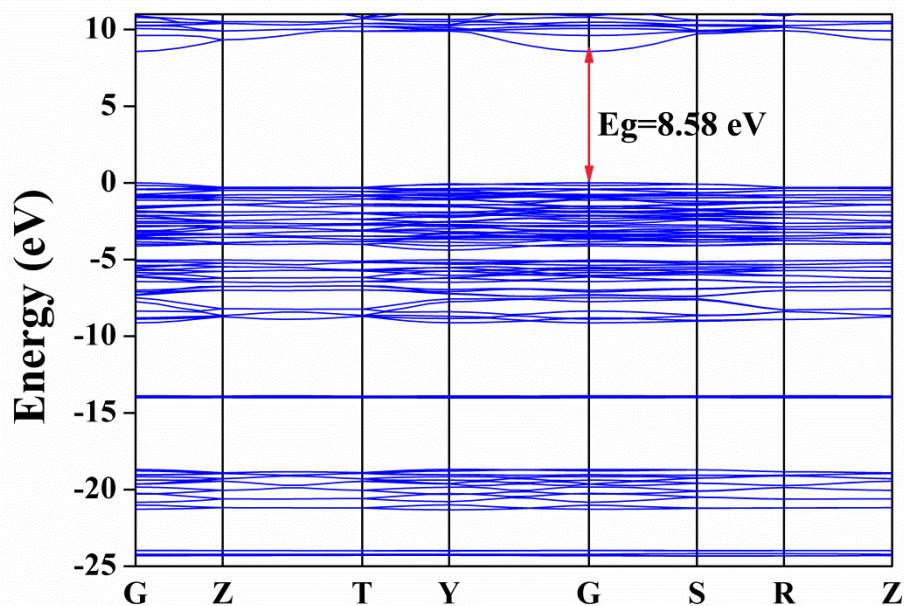**Figure S9.** The UV−vis−NIR spectrum of SrB$_5$O$_7$F$_3$.

**Figure S10**. Electronic band structure of $SrB_5O_7F_3$ based on the results of HSE06 method.



To further explore the band structures and optical properties of $SrB_5O_7F_3$, the related theoretical calculations were carried out by the plane-wave pseudopotential method implemented in the CASTEP package based on DFT.[8] Considering the underestimation of the band gap in standard DFT calculations with GGA owing to the discontinuity of exchange-correlation energy functional, the HSE06 functional has also been performed to ensure the accuracy and consistency of the band gap. The calculated band gaps using GGA and HSE06[9] methods are about 6.89 and 8.58 eV for $SrB_5O_7F_3$, respectively. Although the band gaps calculated by HSE06 match the available experimental values of borates very well (the relative error is less than 5%), GGA usually gives a better description on the optical properties. Therefore, we analyzed optical properties under the GGA framework, and induced a scissor operator (1.69 eV) to shift the conduction bands to agree with the band gap value of HSE06.

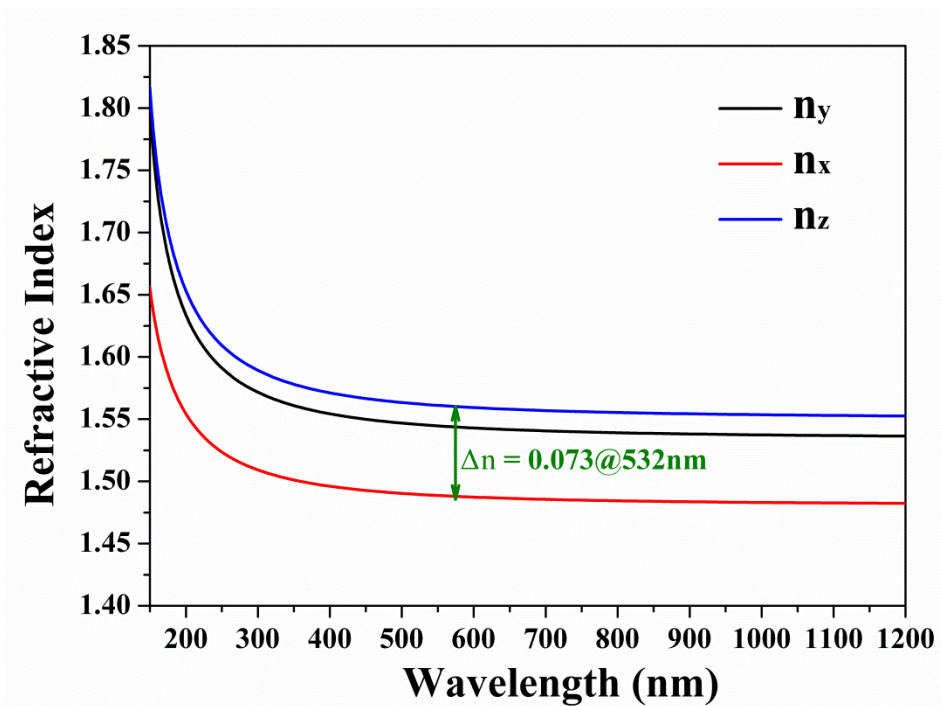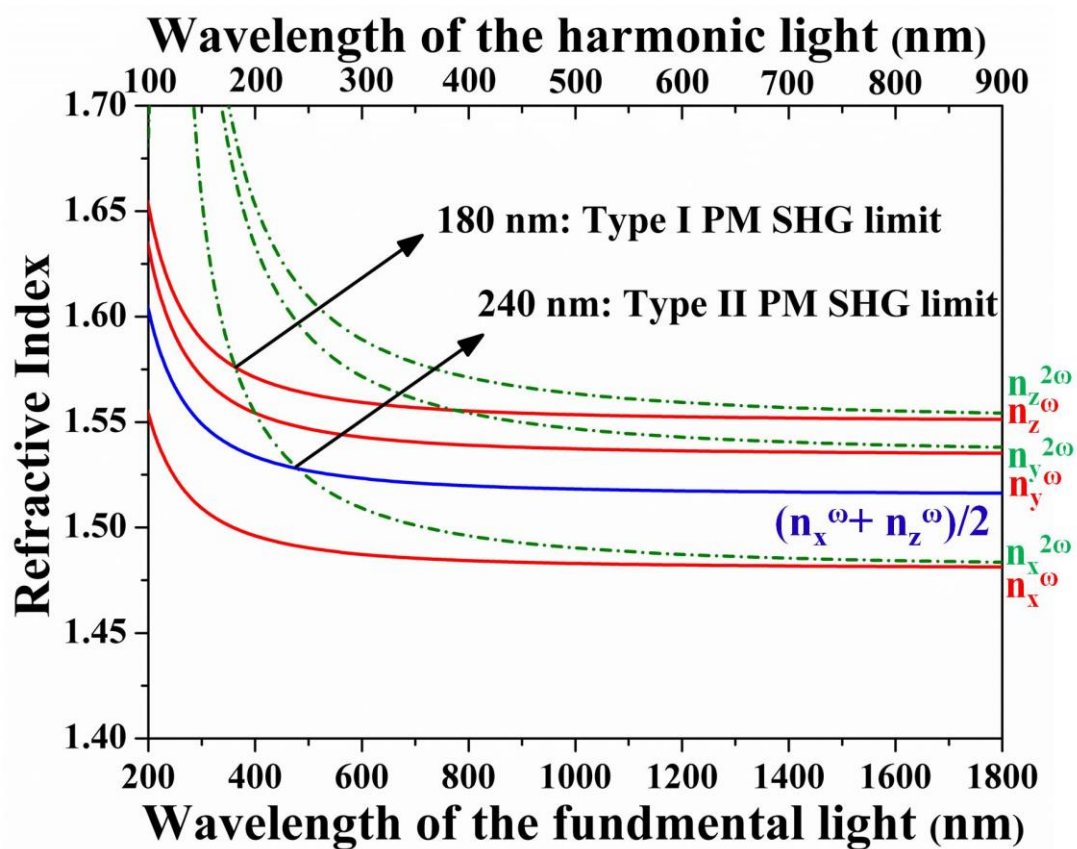**Figure S11**. The calculated refractive indices and birefringence of $SrB_5O_7F_3$.

# References

[1]   SAINT, *Version 7.60A,Bruker Analytical X-ray Instruments, Inc.,Madison, WI,* **2008**.

[2]   Sheldrick, G. M. *SHELXTL, version 6.12; Bruker Analytical X-ray Instruments, Inc.: Madison, WI,* **2001**.

[3]   Spek, A. L.; *J. Appl. Crystallogr.* **2003**, *36*, 7.

[4]   Kurtz, S. K.; Perry, T. T. *J. Appl. Phys.* **1968**, *39*, 3798.

[5]   Clark, S. J.; Segall, M. D.; Pickard, C. J.; Hasnip, P. J.; Probert, M. J.; Refson, K.; Payne, M. C. *Z. Anorg. Allg. Chem.* **2005**, *220*, 567.

[6]   a) Rappe, A. M.; Rabe, K. M.; Kaxiras, E.; Joannopoulos, J. D. *Phys. Rev. B* **1990**, *41*, 1227; b) Lin, J. S.; Qteish, A.; Payne, M. C.; Heine, V. *Phys. Rev. B* **1993**, *47*, 4174; c) Lee, M. H. PhD. Thesis, The University of Cambridge **1996**.

[7]   Perdew, J. P.; Burke, K.; Ernzerhof, M. *Phys. Rev. Lett.* **1996**, *77*, 3865.

[8]   Clark, S. J.; Segall, M. D.; Pickard, C. J.; Hasnip, P. J.; Probert, M. J.; Refson, K.; Payne, M. C. *Z. Kristallogr.* **2005**, *220*, 567.

[9]   (a) Heyd, J.; Scuseria, G. E.; Ernzerhof, M. *J. Chem. Phys.* **2003**, *118*, 8207; (b) Krukau, A. V.; Vydrov, O. A.; Izmaylov, A. F.; Scuseria, G. E. *J. Chem. Phys.* **2006**, *125*, 224106.